Surface Science 603 (2009) 2102–2107

Contents lists available at ScienceDirect

Surface Science

journal homepage: www.elsevier.com/locate/susc

Atomic and electronic structures of thin NaCl films grown on a Ge(0 0 1) surface

Shiow-Fon Tsay [a,*], D.-S. Lin [b]

[a] Department of Physics, National Sun Yat-sen University, No. 70, Lienhai Rd., Kaohsiung, Kaohsiung 80424, Taiwan, ROC
[b] Institute of Physics, National Chiao-Tung University, Hsinchu 300, Taiwan, ROC

ARTICLE INFO

Article history:
Received 6 December 2008
Accepted for publication 2 April 2009
Available online 17 April 2009

Keywords:
Density functional calculations
Semiconductor–insulator interfaces
Alkali halides
Germanium
Surface structure
Thin film structures
Surface electronic phenomena

ABSTRACT

Density functional theory (DFT) with LDA and GGA have been employed to study the interface and thin film properties of NaCl on a Ge(0 0 1) surface. The atomic and electronic structures of thin NaCl films from one to ten monolayers were analyzed. The layer adsorption energies show that a quasi-crystalline (0 0 1) fcc NaCl film is built up via a layer-by-layer growth mode with NaCl thickness above 2 ML. Simulated STM images show a well-resolved (1×1) NaCl atomic structure for sample bias voltage $V_s < -2.5$ V and the bright protrusions should be assigned to the Cl^- ions of the NaCl film. The Ge substrate dimer is reserved and buckled like a clean Ge(0 0 1)-$p(2 \times 2)$ surface as the result of weak interface interaction between the dangling bonds coming from valence π states of the Ge substrate and the 3p states of the interfacial Cl^- ion. These results are consistent with the experiments of STM, LEED and EELS.

1. Introduction

The nature of the solid–solid interface between very dissimilar materials (heterointerface) has become a subject of special interest in condensed matter physics, since novel atomic and electronic structures appear at the interface. Growth of ultrathin epitaxial insulating film and the possibilities to structure these films using a self-organized process is highly important. On both semiconductors and metals, such layers will be needed to separate conducting material in the ultra-small electronic devices of the future. In addition, alkali halides are often regarded as the model structure for both testing experimental methodologies and validating new theories. Thus, thin alkali halide films on semiconductors [1–18] (e.g. KCl/Si [2], CaF_2/Si [3–5], NaCl/Ge [6–13], etc.) or on metals [14–18] (e.g. NaCl/Ag [14], KCl/Cu [15], KCl/Ag [16], LiCl/Cu [17], NaCl/Cu [17], NaCl/Al [18], etc.) have been regaining technological interest recently, as they are relevant for both their electronic and catalytic properties. The interesting problems include growth mechanics, atomic and electronic structures and interface states. It also seems to affect surface color center generation [19].

Thin NaCl films can be grown epitaxially on Ge(0 0 1) with a high degree of quality under appropriate conditions [6–13] due to the small mismatch of only 0.5% of the NaCl (5.63 Å) and Ge (5.66 Å) [20] lattice constants. Therefore, NaCl/Ge(0 0 1) is an ideal candidate for studying the mechanisms of ionic/covalent heteroepitaxy. A wide range of experimental studies [6–13] of NaCl on Ge(0 0 1) have been carried out. The remarkable and unique growth mode ('carpet mode') is suggested for NaCl film of 3–8 double layers of thickness by high-resolution low-energy electron diffraction (LEED) studies [10]. Experimental results also suggest that the subsequent growth of NaCl on the modified surface occurs through the formation of islands with the thickness of a triple-layer, which is filled in until the triple-layer is complete [6]. A well-resolved square lattice with a lattice constant of 4.0 Å STM image is observed, and Glöckler et al. suggested that only one type of ion (Na^+ or Cl^-) of the NaCl(0 0 1) plane is imaged as white protrusions of STM [12]. On the other hand, the NaCl–Ge interface should play an important role in the growth mode, but only a few experiments have studied the properties of buried interfaces [8,11,13]. This is due to the instability of the surface of alkali halides during electron irradiation. Lucas et al. found that the $c(4 \times 2)$ surface reconstruction, the characteristic of clean Ge(0 0 1) at low temperatures, is suppressed immediately upon deposition of NaCl [6]. However, the (2×1) symmetry of the surface unit cell is preserved, even after 6 monolayers (ML) of NaCl have been grown. Zielasek et al. studied the electronic states located at the NaCl–Ge(0 0 1) interface by electron energy loss spectroscopy (EELS), and provided evidence that the dimerization of the Ge(0 0 1) surface is not removed after NaCl deposition [13].

Several problems concerning the structural and electronic properties of this system such as atomic adsorption sites, charge transfer of interfaces, and the nature of the interface are under debate. Until now, the theoretical models lack a complete description of the epitaxial growth mechanism. In this paper the growth mode of NaCl films on a Ge(0 0 1) surface with thicknesses of up to

* Corresponding author. Tel.: +886 7 5253728; fax: +886 7 5253709.
E-mail address: tsaysf@facmail.nsysu.edu.tw (S.-F. Tsay).

0039-6028/$ - see front matter © 2009 Elsevier B.V. All rights reserved.
doi:10.1016/j.susc.2009.04.007

10 ML was studied according to density functional theory (DFT) within local-density approximation (LDA) and generalized gradient approximation (GGA), respectively. The atomic and electronic structures of the NaCl–Ge interface are also presented. The results of the layer adsorption energies suggest a layer-by-layer growth mode beyond two NaCl monolayers. A quasi-crystalline (0 0 1) fcc NaCl film is constructed with a well-resolved (1×1) filled-state simulated STM image as sample bias voltage $V_s \leqslant -2.5$ V. Besides, the Ge substrate dimer is reserved and buckled like a clean Ge(0 0 1)-$p(2 \times 2)$ surface. These results are consistent with the experimental observations. In the band structure calculation, the electronic states located at the interface of NaCl/Ge were clearly observed as the result of coupling the dangling bonds coming from valence π states of the Ge substrate and the 3p states of the interfacial Cl^- ion. However, the coupling strength of the interface states is weak, so the growth mode of the NaCl layer in a (1×1) registry is not affected after 2 ML NaCl deposition. The surface states of Ge providing the band gap states for the wide band gap of alkali halide are found to be similar to the metal induced gap states (MIGS) of insulator/metal interfaces [16].

2. Method

The calculations of total energy were performed using VASP code [21–23] within LDA/GGA approximation of DFT. The Ceperley–Alder exchange-correlation function [24] as parameterized by Perdew and Zunger [25] for LDA and the Perdew–Burke–Ernzerhof (PBE) exchange-correlation function [26–28] for GGA were adopted, respectively. A repeated-slab supercell model was employed. Each slab includes ten atomic layers of Ge and the adlayers of Na and Cl; H atoms were attached to the bottom-layer Ge atoms to saturate their dangling bonds. The heights of the supercell in the [0 0 1] direction were fixed at 60 Å, which was sufficiently large to prevent coupling between the slabs, even for the Na, Cl and H adsorbed on both Ge surfaces. The wave functions were expanded using a plane-wave basis with cutoff energy of 25.72 Ry (350 eV) and a larger cutoff energy (500 eV) to test coverage. The electron-ion interaction pseudopotentials supported by VASP were specified using the projector-augmented wave (PAW) method [29] in which the 2p and 3s electrons of the Na atom, the 3s and 3p electrons of the Cl atom, and the 3d, 4s and 4p electrons of the Ge atom are considered as valence. The calculated lattice parameter of bulk Ge was determined as 5.621 Å for LDA and 5.753 Å for GGA which have a 0.6% and 1.6% error when compared with the experimentally determined value, 5.658 Å, respectively. The GGA result is larger than the experimental one due to the understanding within the DFT–GGA treatment. An 8×8 (4×4) k Monkhorst and Pack mesh, equivalent to 32 (8) irreducible k points, was used to sample the surface Brillouin zone of a 2×2 (4×4) unit cell. By fixing the bottom double Ge and H layers, the structure was optimized until the residual force acting on each atom was less than 0.01 eV/Å.

3. Results

3.1. The clean Ge(0 0 1) surface

The clean Ge(0 0 1) surface consists of buckled dimers, and its buckling orientation alternates along the dimer-row direction (perpendicular to the dimer-axis) like a clean Si(0 0 1) surface. Two kinds of arrangements of the buckled dimers are known to be stable on the surface. One is the $c(4 \times 2)$ structure and the other is $p(2 \times 2)$. The neighboring dimer rows in the $p(2 \times 2)$ structure are buckled in phase while the $c(4 \times 2)$ structure has out of phase buckling. We found that the $c(4 \times 2)$ structure is slightly more stable than the $p(2 \times 2)$ structure by 4.4 meV/dimer for LDA and 42.4 meV/dimer for GGA. The former is consistent with the findings of Yoshimoto et al. [30]. Because the energy difference is so small, an order-disorder phase transition of the buckling orientation occurs around 200 K [31] and a phase transition by carrier injection using STM [32,33] as Si(0 0 1) surface [34] was observed. Above 200 K, the buckling orientation changes so rapidly that the observed structure by STM is (2x1). The calculated dimer length of the $c(4 \times 2)$ structure is 2.51 Å/2.57 Å with a buckling angle of 19.8°/19.5° for LDA/GGA, which is slightly different from the experimental results, 2.46 Å and 17.4° [35].

3.2. 1 ML NaCl on Ge(0 0 1)

Because the $p(2 \times 2)$ and $c(4 \times 2)$ structures of a clean Ge(0 0 1) surface are nearly degenerate in energy, the NaCl was deposited separately on *those two* Ge structure surfaces to study the optimized NaCl/Ge(0 0 1) reconstruction structure. The surface structures of one monolayer of NaCl deposited on clean Ge-$p(2 \times 2)$ surfaces are shown in Fig. 1a and b, respectively, and that on Ge-$c(4 \times 2)$ surface is shown in Fig. 1c. The most stable optimized NaCl reconstruction is a (2×2) structure as shown in Fig. 1a (denoted as A1). This reconstruction structure is more stable than the other two surface structures, (2×2) and $c(4 \times 2)$ (denoted as A2 and A3) by 270 and 273 meV per 2×2 supercell for LDA, respectively, which are shown in Fig. 1b and c. For the 2×2 superstructure of the A1 structure, two Cl atoms [Cl(1)] reside on the top (T) of the dimer down Ge atom, and the other two Cl atoms [Cl(2)] abide between the T and Valley bridge (VB) sites. Each Cl(2) assembles the surrounding three Na ions and constitutes an Na_3Cl triangular-cluster. One of three Na^+ ions, Na(1), is near the pedestal (P) site and the other two, Na(2) and Na(3), lie between the cave (C) and VB sites. The corresponding positions of the T, VB, P, C and bridge (B) sites are shown in Fig. 1b. The Na_3Cl triangular clusters are lined along the dimer-row direction, and form a double-layer-like structure as displayed in the side view of Fig. 1a. Cl(1) and

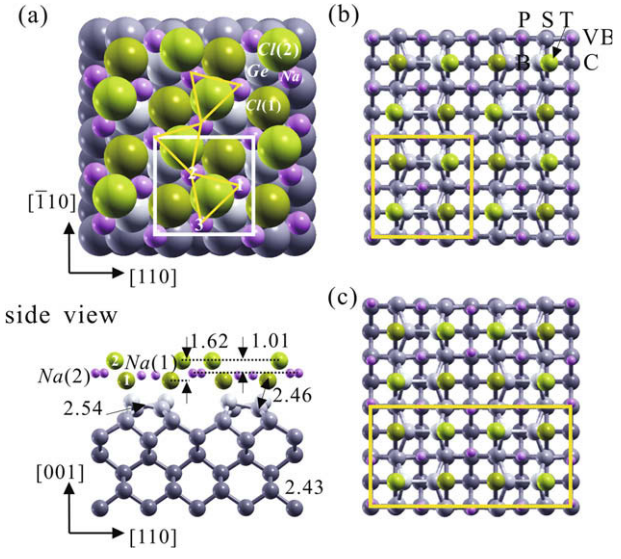

Fig. 1. Top view of three atomic structures, (a) A1, (b) A2 and (c) A3 for the Ge(0 0 1) surface covered with 1 ML of NaCl. The top and side views of the A1 structure are also shown in (a). The VB, B, C, P, S and T are denoted as the Valley bridge, bridge, cave, pedestal, shallow sites and top of dimer, respectively. The green, violet and silver solid spheres represent the Cl, Na and Ge atoms, respectively. The dark colored spheres represent the deeper atoms from the surface. Some bond lengths and the layer distances for LDA are displayed in (a). The unit of length is angstrom. (For interpretation of the references to colour in this figure legend, the reader is referred to the web version of this article.)

Cl(2) have a large height difference of 1.617 Å, while the Na(1) and Na(2) ions have a small height difference of 0.180 Å for LDA. The inter-atomic distances of Na(2)–Cl(2) and Ge–Cl(1) are 2.575 ± 0.011 and 2.459 ± 0.001 Å, respectively. The corresponding atomic distances for GGA are also listed in Table 1. The Na atoms of the A2 and A3 structures are located at both VB and P sites which are the two most stable sites for sub-monolayer Na adsorbed on a clean Ge(0 0 1) surface. Chlorine atoms are located at the top of dimers and arrange as $p(2 \times 2)$ and $c(4 \times 2)$ structures, A2 and A3, respectively, depending on the buckling mode of Ge dimers. Even though the $c(4 \times 2)$ structure is more stable than the $p(2 \times 2)$ structure for a clean Ge(0 0 1) surface, the energy of the A2 structure is lower than that of the A3 structure as a result of short neighboring chlorine's distances in the A3 structure. These results show that the phase transformation of the Ge substrate from $c(4 \times 2)$ to $p(2 \times 2)$ could be induced by the NaCl deposition and also imply that the adsorbate–adsorbate interactions could be the key factor to determine the system's energy, rather than the adsorbate–substrate interaction.

For the optimal A1 structure, the dimers also display a $p(2 \times 2)$ structure, but the bond length extends to 2.54 Å/2.59 Å with a buckling angle of 13.1°/12.8° for LDA/GGA; i.e., the Ge atoms of each dimer have a height difference of 0.59 Å which is smaller than that of a clean Ge(0 0 1) surface. It is indicated that the Ge dimer rows survive after adsorption of NaCl, whereas the $c(4 \times 2)$ structure is suppressed immediately upon NaCl deposition. Therefore, a modified (2×1) reconstruction at the interface was observed as shown in the X-ray scattering data [6] resulting from the thermal flipping.

3.3. 2 ML NaCl on Ge(0 0 1)

The optimized atomic arrangements ultimately display the same 2×2 double-layer NaCl reconstruction as shown in Fig. 2 no matter where the second NaCl monolayer was deposited on the A1 or A2 structures. This optimized atomic structure is different from the model suggested by Lucas et al. [6] in which the Ge remains and sodium is adsorbed in the valley site. Notably, the optimized atomic positions for Na and Cl ions are significantly different from those of 1 ML NaCl/Ge(0 0 1). The Na ions are located around the shallow-sites (S, or inter-dimer-bridge) on the first NaCl layer with displacement by Δy and Δx as listed in Table 1 along [1 $\bar{1}$ 0] and [1 1 0] directions. The Cl ions are located around the C and B sites and shift the same order of magnitude of displacement as that of the Na ions. The Na^+ and Cl^- alternatively arrange

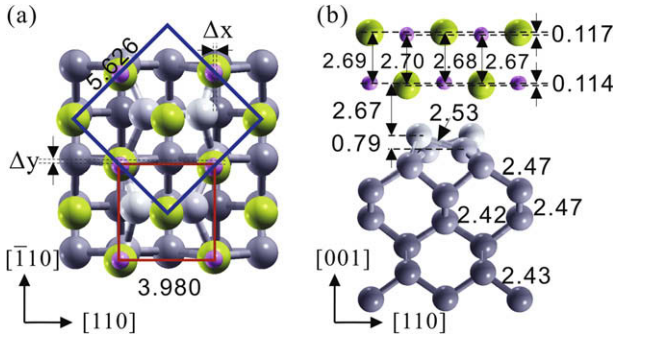

Fig. 2. The (a) top and (b) side views of the optimal structure of 2 ML NaCl/Ge(0 0 1). Some bond lengths and the layer distances for LDA are displayed. The unit of length is angstrom.

in [1 0 0], [0 1 0] and [0 0 1]; thus, an [0 0 1] fcc NaCl double-layer structure is formed. The intra-layer Na–Cl distance is 2.813 Å for LDA (2.879 Å for GGA), which is in agreement with the nearest neighbor separation of an ideal NaCl crystal, 2.820 Å, and the experimental cubic lattice constant of a = 5.65 Å [20]. The inter-layer Na–Cl distance along the [0 0 1] direction has small fluctuations within the range of 2.67–2.70 Å for LDA as shown in Fig. 2b, which is smaller than that of the intra-layer. Within the intra-layer, the Na and Cl ions have small height differences Δh, $\Delta h = h_{Na} - h_{Cl}$, −0.117 Å for the top layer and +0.114 Å for the bottom layer. The interfacial chlorine ions are always outward; therefore, surface polarization occurs on both interfaces of the NaCl thin film.

The nearest inter-atomic distances of Cl(1)–Ge and Na(1)–Ge are 3.409 Å and 3.152 Å for LDA and 3.826 Å and 3.644 Å for GGA, respectively, which are larger than those of 1ML NaCl/Ge(0 0 1). This implies that the interaction between adsorbate and substrate weakens with an increase in the coverage of NaCl (Θ_{NaCl}) on the growth of NaCl film. On the other hand, the Ge dimer layer is reserved as a 2×2 structure with a length of 2.53 Å and 18.2° buckling for LDA and 2.57 Å and 19.2° for GGA, respectively; these parameters are close to those of the clean Ge(0 0 1) surface. Therefore, the bonding of the interface between the NaCl layer and the Ge(0 0 1) surface should be rather weak for the 2 ML NaCl/Ge(0 0 1) surface. It is noted that there are extraordinary discrepancies (about 10%) between LDA and GGA (PBE and PW91) for the Cl–Ge and Na–Ge distances, which remain even with a stricter convergence criterion. The magnitudes of the discrepancy

Table 1
The relative characteristic parameters of clean Ge(0 0 1), 1 ML and 2 ML NaCl/Ge(0 0 1) surfaces within LDA and GGA. Here, $d_{Cl(1)-Ge}$, $d_{Cl(2)-Ge}$, $d_{Na(1)-Ge}$, and $d_{Na(2)-Cl(2)}$ are the atomic distances for Cl(1)–Ge, Cl(2)–Ge, Na(1)–Ge and Na(2)–Cl(2); $h_{Na(2)-Cl(2)}$, $h_{Na(1)-Na(2)}$ and $h_{Cl(1)-Cl(2)}$ are the height distances for Na(2)–Cl(2), Na(1)–Na(2) and Cl(1)–Cl(2) along the [0 0 1] direction. Δx and Δy are the Na or Cl position shifts of the NaCl layer relative to the Ge substrate along [1 1 0] and [$\bar{1}$ 1 0] directions, respectively, as shown in Fig. 2. $Na-Cl|_{\perp[0\,0\,1]}$ and $Na-Cl|_{//[0\,0\,1]}$ are the intra-layer and inter-layer Na–Cl distances, respectively.

	Clean Ge(0 0 1)		1 ML NaCl/Ge(0 0 1)		2 ML NaCl/Ge(0 0 1)	
	LDA	GGA	LDA	GGA	LDA	GGA
a_0 (Å)	5.621	5.753				
Dimer length (Å)	2.513	2.571	2.541	2.594	2.527	2.571
Buckling angle	19.8°	19.5°	13.1°	12.7°	18.2°	19.2°
$d_{Cl(1)-Ge}$ (Å)			2.459	2.575	3.409	3.826
$d_{Cl(2)-Ge}$ (Å)			3.828	4.104	3.544	4.019
$d_{Na(1)-Ge}$ (Å)			3.036	3.075	3.152	3.644
$d_{Na(2)-Cl(2)}$ (Å)			2.575	2.624		
$h_{Na(2)-Cl(2)}$ (Å)			1.008	0.988		
$h_{Na(1)-Na(2)}$ (Å)			0.180	0.404		
$h_{Cl(1)-Cl(2)}$ (Å)			1.617	1.882		
Δx (a_0)					0.011	0.026
Δy (a_0)					0.062	0.030
$Na-Cl\|_{\perp[0\,0\,1]}$ (Å)					2.813	2.879
$Na-Cl\|_{//[0\,0\,1]}$ (Å)					2.67–2.70	2.77–2.80

depend on the use of exchange-correlation functions as the layer adsorption energies which are shown in Fig. 3.

3.4. $\Theta_{NaCl} \geqslant 3$ ML

Because of weak coupling between the substrate and the NaCl layer, more NaCl can be deposited layer by layer without much change to the Ge–NaCl interface. The NaCl layers up to 10 ML of thickness have been studied in this work. The NaCl film is flat except for small height fluctuations between the Na^+ and Cl^- ions at the film/vacuum and film/substrate interfaces, similar to the case of 2ML NaCl/Ge. The interfacial Cl^- ions are always further out than the Na^+ ions, no matter whether they are on the vacuum side or the substrate side. For LDA, the calculated dimer length of 2.53 Å with a buckling angle of 17.9° is retained with the thickness of NaCl up to 10 ML. These values are compatible with those of $\Theta_{NaCl} = 2$ ML, implying that the grown NaCl film on a Ge(0 0 1) surface beyond 2 ML resembles that of NaCl crystal. This is consistent with the experimental results which show the sharpest LEED patterns when the NaCl films grow on Ge(0 0 1) [7], and a modified (2×1) reconstruction at the interface remains [6].

4. Discussion

To find a plausible growth model of NaCl on a Ge(0 0 1) surface, the layer adsorption energies per adatom pair of Na and Cl, $\Delta E_{ads}(n)$ were calculated as shown in Fig. 3 for LDA and GGA, which are the released energies per Na and Cl atoms adsorbed on an $(n-1)$ ML NaCl/Ge(0 0 1) surface, and are defined as

$$\Delta E_{ads}(n) = [E_{NaCl/Ge}(n-1) + E_{Na} + E_{Cl} - E_{NaCl/Ge}(n)],$$

where $E_{NaCl/Ge}(n)$ is the total energy of n-ML NaCl adsorbed on a Ge(0 0 1) surface, and n denotes the coverage of NaCl which also corresponds to the thickness of the NaCl overlayer for $n \geqslant 1$. $E_{NaCl/Ge}(0)$ corresponds to the clean Ge(0 0 1) surface. E_{Na} and E_{Cl} are the total energies of spin-polarized free Na and Cl atoms, respectively. Fig. 3 shows that the layer adsorption energies strongly depend on the exchange-correlation function, but $\Delta E_{ads}(n)$ is almost independent of the thickness of the NaCl layer when $\Theta_{NaCl} > 3$ ML, no matter what kinds of exchange-correlation functions were adopted. Therefore, NaCl grown on the Ge(0 0 1) surface firstly builds as a double-layer island (or cluster), then layer by layer for a coverage of NaCl greater than 3 ML. Our results support the double-single-layer growth model as suggested by Refs. [10,12], and also explain the triple-layer growth model of Ref. [6] with an initial layer thickness of about 8.3 Å (corresponding to 3 ML) under suitable evaporation rates, but which were too fast to allow observation of the initial growth of the double layer thickness island.

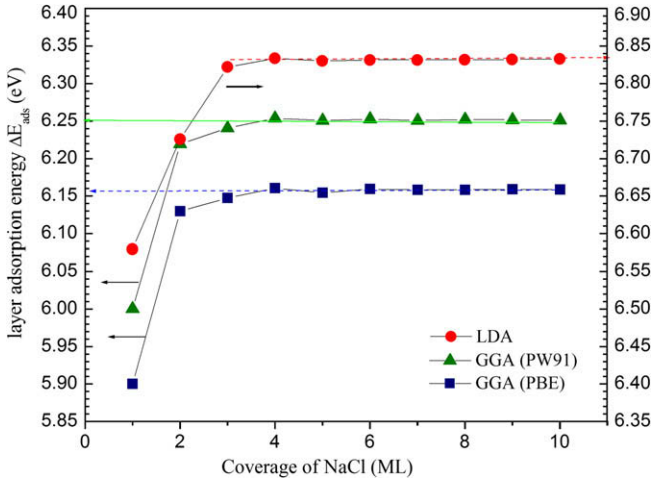

Fig. 3. The layer adsorption energies per 1×1 supercell for NaCl adsorbed on a Ge(0 0 1) surface for LDA and GGA approximations. The Perdew–Burke–Ernzerhof (PBE) and Perdew–Wang 91 (PW91) exchange-correlation functions for GGA were adopted, respectively.

In order to estimate the thickness of NaCl layers, the average layer charge densities along the [0 0 1] direction for various NaCl coverages and their gradient within LDA are shown in Fig. 4. The heights of 1 ML and 2 ML NaCl relative to the clean Ge(0 0 1) surface were estimated from the part of the parallel line behavior of $d[ln\rho(z)]/dz$, which are 3.650 ± 0.285 Å and 5.843 ± 0.394 Å for LDA, respectively. Therefore, the lateral height of the first (double layer) and the second (single) ML of NaCl are considered as 3.650 and 2.193 (=5.843 − 3.650) Å, respectively. These values are in agreement with the STM results [11] 3.8 ± 0.3 Å for the first (double) and 2.0 ± 0.3 Å for the second (single) NaCl layers, and within the range of reasonable deviations. The deviations could be attributed to the fact that the tunneling barrier is not only determined by the vacuum between the tip and the NaCl layer, but also by the NaCl layer itself. The lateral height of the STM scan could also be influenced by the sample-tip interaction. In addition, above the second ML, the height distances between any two nearest neighboring NaCl overlayers are 2.668–2.719 Å, which is consistent with the experimental observations.

According to the Tersoff–Hamann approximation, the tunneling current in STM is proportional to the local density of states (LDOS) near the Fermi level at the position of the tip. To account for the STM tunneling current, we integrate the LDOS between the sample bias and the Fermi energy level. The partial density $\rho^{STM}(r) = \int_{E_F+eV_s}^{E_F} dE \sum_{n\mathbf{k}} |\psi_{n\mathbf{k}}(\mathbf{r})|^2 \delta(E - \varepsilon_{n\mathbf{k}})$ should reflect the STM tunneling currents. Fig. 5 shows the simulated filled-state STM images above the top NaCl layer by 1.5 Å at various sample voltages for 2 ML NaCl/Ge(0 0 1). The images display 1×1 images for $V_s \leqslant -2.5$ V, and 2×2 images for $V_s > -2.0$ V. The 1×1 image is consistent with a well-resolved square lattice observation with a lattice constant of 4.0 Å experimentally at $V_s = -2.7$ V [12]. It also reveals that the bright protrusions of the filled-state STM image at a sample bias of $|V_s| \geqslant 2.5$ V should be assigned to the Cl^- ions of the top NaCl film, and excludes the possibility of coming from Na^+ ions as reported by Ref. [12]. This result was also confirmed by the band structure calculations in the following discussion.

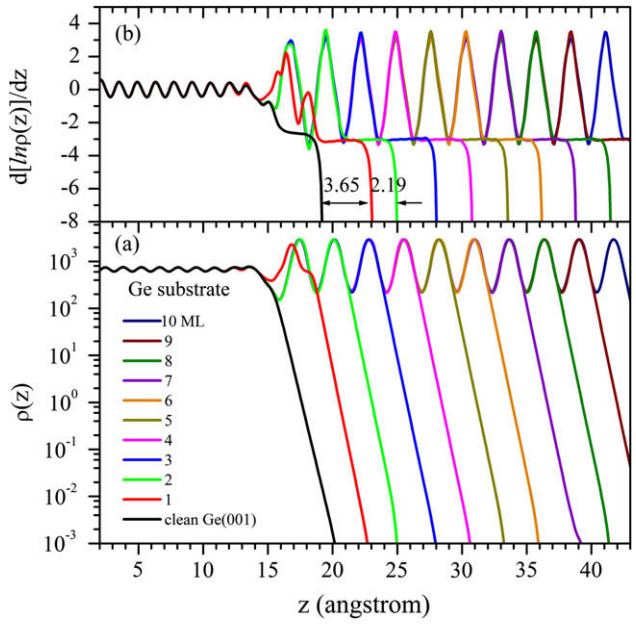

Fig. 4. (a) The average layer charge densities along the [0 0 1] direction for various NaCl coverages and (b) their deviations within LDA.

The valence state of Na is nearly empty to contribute efficiently to the tunneling current at or near −2.7 V sample voltage. Fig. 5 also shows that the bright protrusions of LDOS approach to the neighboring dimer up-Ge atoms when the sampling voltage decreases; then the image of 1×1 bright protrusions changes to a 2×2 image. In order to explore what kinds of states contribute to these STM images, the surface band structures were calculated. However, the intensity of the image at V_s = −1.0 V is weaker by three orders of magnitude than that at V_s = −3.0 V as shown in Fig. 5.

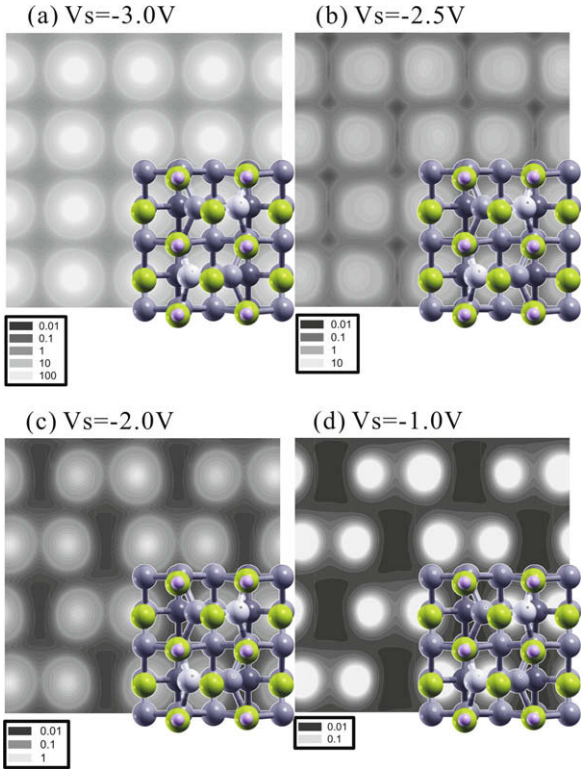

Fig. 5. The simulated STM images for 2 ML NaCl/Ge(0 0 1) surface above the top NaCl overlayer by 1.5 Å with different sample bias at (a) −3.0 V, (b) −2.5 V, (c) −2.0 V and (d) −1.0 V.

Fig. 6 shows the electronic band structure and the total density of states (DOS) around the Fermi energy level for the 10 ML NaCl/Ge(0 0 1) system. Above the Fermi energy level (E_F), the dangling bond π^* state is clear within the gap. It displays a quasi-one-dimensional behavior with small dispersion along the dimer-axis direction, $\overline{\Gamma J}$, and largely disperses in the dimer-row direction, $\overline{\Gamma J'}$. This is consistent with that of the clean Ge(0 0 1) surface clarified recently both experimentally and theoretically [30,33.36]; therefore, the π^* state was hardly influenced when the NaCl was adsorbed on the Ge(0 0 1) surface. Below the Fermi energy level, the S1 states couple the dangling-bond valence π states of the Ge surface and the 3*p* states of the interfacial Cl^- ion in the region of E_F to E_F −1.0 eV. The isosurface of charge density distribution of S1 states with 0.03 $e/Å^3$ are shown in Fig. 7. The charge contours, in the range of 0.00–0.075 with spacing of 0.0025 $e/Å^3$, on the planes sliced at the Cl^- ion along the dimer-axis and the dimer-row directions are also shown in Fig. 7a and b, respectively. It is noted that the charge density distribution of the interface S1 states

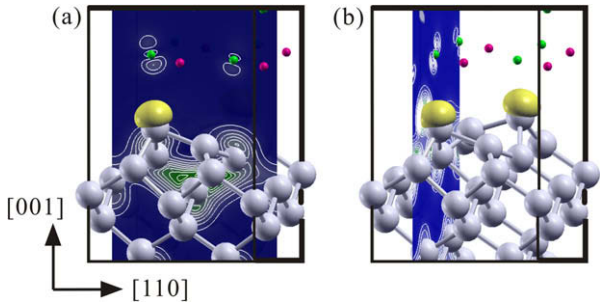

Fig. 7. The charge density distribution of the interface S1 bands of 10 ML NaCl/Ge(0 0 1). The isosurface represents 0.03 $e/Å^3$. The charge contour lines, in the range from 0.00 to 0.075 with spacing of 0.0025 $e/Å^3$, on the slices cut at Cl^- ion viewing along the (a) dimer-axis and (b) the dimer-row directions. The green, violet and silver solid spheres represent Cl, Na and Ge atoms, respectively. (For interpretation of the references to colour in this figure legend, the reader is referred to the web version of this article.)

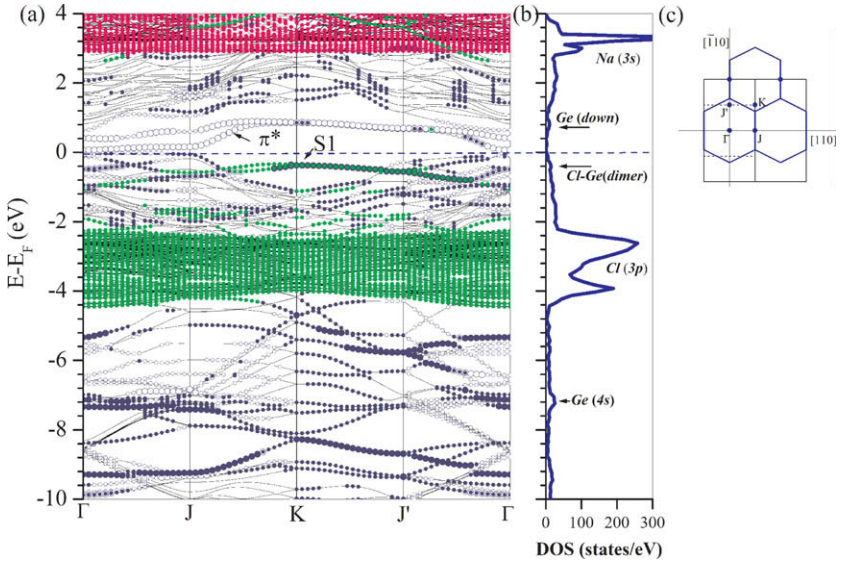

Fig. 6. (a) The electronic band structure and (b) LDOS for 10 ML NaCl/Ge(0 0 1) surface surrounding the Fermi level. The axes are defined for the 2×2 surface Brillouin zones as in (c). *J* is defined as the point in the dimer-axis direction and *J'* as that in the dimer-row direction for the (2×2) surface Brillouin zones. The states corresponding to the Na and Cl are indicated by pink and green solid circles, respectively, and that of the dimer up-Ge and down-Ge are represented by the full and empty blue circles, respectively. The surface S1 and π^* bands are indicated. (c) The surface Brillouin zones for the (2×1) (thin lines), $p(2 \times 2)$ (dotted lines) and $c(4 \times 2)$ (thick lines) surfaces. (For interpretation of the references to colour in this figure legend, the reader is referred to the web version of this article.)

is indeed localized at the dimer up-Ge atom and the interfacial Cl^- ion. Therefore, the LDOS of the dimer up-Ge atom and the polarized Cl^- ions results in a 2×2 simulated STM image as shown in Fig. 5c and d. The interface states originating from the wave function of the dimer up-Ge atom penetrating into an insulating side at the alkali halide/semiconductor interface is similar to the metal induced gap states (MIGS) of the insulator/metal interfaces [16]. The adsorbate-induced surface states within the forbidden band gap of the NaCl and KCl are observed by UPS and EELS after water or salicylic acid adsorption (see Figs. 3–5 of Ref. [8]).

Fig. 6 also shows that the 3*s* bands of Na (pink solid circles) are located above the Fermi energy level by 2.91 eV with a maximum LDOS at 3.29 eV; this demonstrates that the Na^+ is a perfect ionic, and displays a closed shell charge distribution in the NaCl thin film. In contrast, the density of Cl *3p* states distribute below the Fermi energy level in the energy range of 2.25–4.43 eV at Γ point. Its corresponding LDOS has two main peaks; one is about 2.61 eV and the other is about 3.90 eV, and the intensity of the latter is about one-half of the former. Experimentally, EELS occurring at around 2.6 eV was observed for different thicknesses of the NaCl film on a Ge(0 0 1) surface [13,19]. This can be attributed to the excitation of the chlorine *3p* states of the NaCl-capped on Ge(0 0 1).

5. Conclusion

The atomic structures, electronic structures and interfacial properties of thin NaCl films grown on a Ge(0 0 1) surface were studied by the DFT within LDA and GGA. The layer adsorption energies and the optimal structures indicate a double-layer growth mode for the coverage of NaCl less than 1 ML, and a layer-by-layer growth mode for coverage over 2 ML. This is consistent with the double-single-layer growth model suggested by experiments [7,12]. A quasi-crystalline (0 0 1) fcc NaCl layer is built up when $\Theta_{NaCl} \geqslant 2$ ML. The clear (1×1) simulated filled-state STM images as sample bias voltage $V_s \leqslant -2.5$ V present the 3*p* state of Cl^- ions of the NaCl overlayer, which is consistent with the STM results. The surface S1 states indicate that a very weak coupling between the interfacial Cl^- ions and the dimer up-Ge atom results in a very weak (2×2) filled-state STM image as $V_s \sim -1.0$ V. However, the interfacial Ge atomic layer reserves its buckling angle with little length dilation after NaCl adsorption. The adsorbate-adsorbate interaction only strongly dominates the structure of the NaCl film of less than two monolayers in thickness. The electronic structures of the NaCl/Ge(0 0 1) are almost the same when the coverages of NaCl are more than 2 ML, which is consistent with the experimental observations. The photoemission spectra of NaCl are indistinguishable from those of thicker layers once a well ordered two layers of NaCl has grown [8–10]. These calculation results are consistent with the results of LEED, STM, and EELS experiments [10,12,13].

Acknowledgments

This work is supported by the National Science Council of Taiwan under Contract No. NSC 95-2112-M-110-016-MY3 (SFT) and NSC 95-2112-M009-0039-MY4 (DSL). S.-F. Tsay also acknowledges the computing resources of NCHC and the Center for Nanoscience and Nanotechnology of NSYSU.

References

[1] R. Bennewitz, J. Phys.: Condens. Matter 18 (2006) R417.
[2] S.-F. Tsay, J.Y. Chung, M.-F. Hsieh, S.-S. Ferng, C.-T. Lou, D.-S. Lin, Surf. Sci. 603 (2009) 419.
[3] J.L. Batstone, J.M. Phillips, E.C. Hunke, Phys. Rev. Lett. 60 (1988) 1394.
[4] R.M. Tromp, M.C. Reuter, Phys. Rev. Lett. 61 (1988) 1756.
[5] A. Klust, T. Ohta, A.A. Bostwick, Q. Yu, F.S. Ohuchi, M.A. Olmstead, Phys. Rev. B 69 (2004) 035405.
[6] C.A. Lucas, G.C.L. Wong, C.S. Dower, F.J. Lamelas, P.H. Fuoss, Surf. Sci. 286 (1993) 46.
[7] S. Fölsch, U. Barjenbruch, M. Henzler, Thin Solid films 172 (1989) 123.
[8] U. Barjenbruch, S. Fölsch, M. Henzler, Surf. Sci. 211/212 (1989) 749.
[9] A. Klekamp, E. Umbach, Surf. Sci. 284 (1993) 291.
[10] C. Schwennike, J. Schimmelpfennig, H. Pfnür, Surf. Sci. 293 (1993) 57.
[11] G. Brusdeylines, N.S. Luo, P. Ruggerone, D. Schmicker, J.P. Toennies, R. Vollmer, T. Wach, Surf. Sci. 272 (1992) 358.
[12] K. Glöckler, M. Sokolowski, A. Soukopp, E. Umbach, Phys. Rev. B 54 (1996) 7705.
[13] V. Zielasek, T. Hildebrandt, M. Henzler, Phys. Rev. B 69 (2004) 205313.
[14] J. Kramer, C. Tegenkamp, J. Phys.: Condens. Matter 15 (2003) 6473.
[15] M. Kiguchi, G. Yoshikawa, S. Ikeda, K. Saiki, Phys. Rev. B 71 (2005) 153401.
[16] R. Arita, Y. Tanida, K. Kuroki, H. Aoki, Phys. Rev. B 69 (2004) 115424.
[17] J. Repp, S. Fölsch, Gerhard Meyer, Phys. Rev. Lett. 86 (2001) 252.
[18] W. Hebenstreit, M. Schmid, J. Redinger, R. Podloucky, P. Varga, Phys. Rev. Lett. 85 (2000) 5376.
[19] V. Zielasek, T. Hildebrandt, M. Henzler, Phys. Rev. B 62 (2000) 2912.
[20] C. Kittle, Introduction of Solid State Physics, 7th ed., John Wiley and Sons, New York, 1996 (p. 67).
[21] G. Kresse, J. Hafner, Phys. Rev. B 47 (1993) R558.
[22] G. Kresse, J. Furthmüller, Comput. Mater. Sci. 6 (1996) 15.
[23] G. Kresse, J. Furthmüller, Phys. Rev. B 54 (1996) 11169.
[24] D.M. Ceperley, B.J. Alder, Phys. Rev. Lett. 45 (1980) 566.
[25] J.P. Perdew, A. Zunger, Phys. Rev. B 23 (1981) 5048.
[26] John P. Perdew, J.A. Chevary, S.H. Vosko, Koblar A. Jackson, Mark R. Pederson, D.J. Carlos, Carlos Fiolhais, Phys. Rev. B 46 (1992) 6671;
John P. Perdew, J.A. Chevary, S.H. Vosko, Koblar A. Jackson, Mark R. Pederson, D.J. Singh, Carlos Fiolhais, Phys. Rev. B 48 (1993) 4978E.
[27] J.P. Perdew, in: P. Ziesche, H. Eschrig (Eds.), Electronic Structure of Solids '91, Akademie Verlag, Berlin, 1991, p. 11.
[28] J.P. Perdew, K. Burke, M. Ernzerhof, Phys. Rev. Lett. 77 (1996) 3865.
[29] P.E. Blöchl, Phys. Rev. B 50 (1994) 17953;
G. Kresse, D. Joubert, Phys. Rev. B 59 (1999) 1758.
[30] Y. Yoshimoto, Y. Nakamura, H. Kawai, M. Tsukada, M. Nakayama, Phys. Rev. B 61 (2000) 1965.
[31] S.D. Kevan, N.G. Stoffel, Phys. Rev. Lett. 53 (1984) 702;
S.D. Kevan, Phys. Rev. B 32 (1985) 2344.
[32] Y. Takagi, Y. Yoshimoto, K. Nakatsuji, F. Komori, Surf. Sci. 559 (2004) 1;
Y. Takagi, Y. Yoshimoto, K. Nakatsuji, F. Komori, J. Phys. Soc. Jpn. 72 (2003) 2425;
Y. Takagi, Y. Yoshimoto, K. Nakatsuji, F. Komori, J. Phys. Soc. Jpn. 74 (2005) 3143.
[33] Y. Takagi, K. Nakatsuji, Y. Yoshimoto, F. Komori, Phys. Rev. B 75 (2007) 115304.
[34] K. Sagisaka, D. Fujita, G. Kido, Phys. Rev. Lett. 91 (2003) 146103;
K. Sagisaka, D. Fujita, Phys. Rev. B 71 (2005) 245319;
D. Riedel, M. Lastapis, M. Martin, G. Dujardin, Phys. Rev. B 69 (2004) 121301(R).
[35] R. Rossmann, H.L. Meyerheim, V. Jahns, J. Wever, W. Moritz, D. Wolf, D. Dornisch, H. Schulz, Surf. Sci. 279 (1992) 199.
[36] K. Nakatsuji, Y. Takagi, F. Komori, H. Kusuhara, A. Ishii, Phys. Rev. B 72 (2005) 241308(R).